

# High-phosphate induced vascular calcification is reduced by iron citrate through inhibition of extracellular matrix osteo-chondrogenic shift in VSMCs

Paola Ciceri <sup>a</sup>, Monica Falleni <sup>b</sup>, Delfina Tosi <sup>b</sup>, Carla Martinelli <sup>b</sup>, Gaetano Bulfamante <sup>b</sup>, Geoffrey A. Block <sup>c</sup>, Piergiorgio Messa <sup>a</sup>, Mario Cozzolino <sup>d,\*</sup>

<sup>a</sup> Renal Research Laboratory, Department of Nephrology, Dialysis and Renal Transplant, Fondazione IRCCS Ca' Granda, Ospedale Maggiore Policlinico & Fondazione D'Amico per la Ricerca sulle Malattie Renali, Italy

<sup>b</sup> Department of Health Sciences, Division of Pathology, University of Milan, ASST Santi Paolo e Carlo, Milan, Italy

<sup>c</sup> Nephrology, Denver Nephrologists PC, Denver, CO, USA

<sup>d</sup> Laboratory of Experimental Nephrology, Department of Health Sciences, University of Milan, Italy

## ARTICLE INFO

### Article history:

Received 15 May 2019

Received in revised form

16 August 2019

Accepted 25 September 2019

Available online xxx

### Keywords:

Iron

Vascular calcification

Extracellular matrix

VSMC

Phosphate

## ABSTRACT

**Background:** High serum phosphate (Pi) levels strongly associate with cardiovascular morbidity and mortality in chronic kidney disease (CKD) patients with vascular calcification playing a major role in the pathogenesis of related cardiovascular disease. High-Pi challenged vascular smooth muscle cells (VSMCs) undergo simili-osteoblastic transformation and actively deposit calcium-phosphate crystals. Iron-based Pi-binders are used to treat hyperphosphatemia in CKD patients.

**Methods:** In this study, we investigated the direct effect of iron citrate on extracellular matrix (ECM) modification induced by high-Pi, following either prophylactic or therapeutic approach.

**Results:** Iron prophylactically prevents and therapeutically blocks high-Pi induced calcification. Masson's staining highlights the changes of muscular ECM that after high-Pi stimulation becomes fibrotic and which modifications are prevented or partially reverted by iron. Interestingly, iron preserves glycogen granules and either prevents or partially reverts the formation of non-glycogen granules induced by high-Pi. In parallel, iron addition is able to either prevent or block the high-Pi induced acid mucin deposition. Iron inhibited calcification also by preventing exosome osteo-chondrogenic shift by reducing phosphate load ( $0.61 \pm 0.04$  vs  $0.45 \pm 0.05$ , PivsPi + Fe,  $p < 0.05$ , nmol Pi/mg protein) and inducing miRNA 30c ( $0.62 \pm 0.05$  vs  $3.07 \pm 0.62$ ; PivsPi + Fe,  $p < 0.01$ , relative expression). Studying aortic rings, we found that iron significantly either prevents or reverts the high-Pi induced collagen deposition and the elastin decrease, preserving elastin structure ( $0.7 \pm 0.1$  vs  $1.2 \pm 0.1$ ; Pi vs Pi + Fe,  $p < 0.05$ , elastin mRNA relative expression).

**Conclusions:** Iron directly either prevents or partially reverts the high-Pi induced osteo-chondrocytic shift of ECM. The protection of muscular nature of VSMC ECM may be one of the mechanisms elucidating the anti-calcific effect of iron.

© 2019 Elsevier B.V. All rights reserved.

## 1. Introduction

Vascular calcification (VC) is recognized as one of the main causes of cardiovascular disease and arterial stiffness in end stage

renal disease patients [1]. The pathogenesis of arterial calcification is multifactorial, implicating factors such as plasma constituents maintaining minerals in solution or inducing tissue mineral deposition. Calcium (Ca) and inorganic phosphate (Pi) act synergistically to induce VC. The major mechanism whereby elevated extracellular Ca and Pi drives VSMC calcification is via release of matrix vesicles [2].

A process of mechanical homeostasis between extracellular matrix (ECM) and VSMCs is a fundamental concept in VC and arterial stiffness [3]. The role of ECM proteins, mainly the elastic

\* Corresponding author. Renal Division and Laboratory of Experimental Nephrology, Dipartimento di Scienze della Salute, Università di Milano, Renal Division, S. Paolo Hospital, Milan, Via A. di Rudini, 8, 20142, Milan, Italy.

E-mail address: [mario.cozzolino@unimi.it](mailto:mario.cozzolino@unimi.it) (M. Cozzolino).

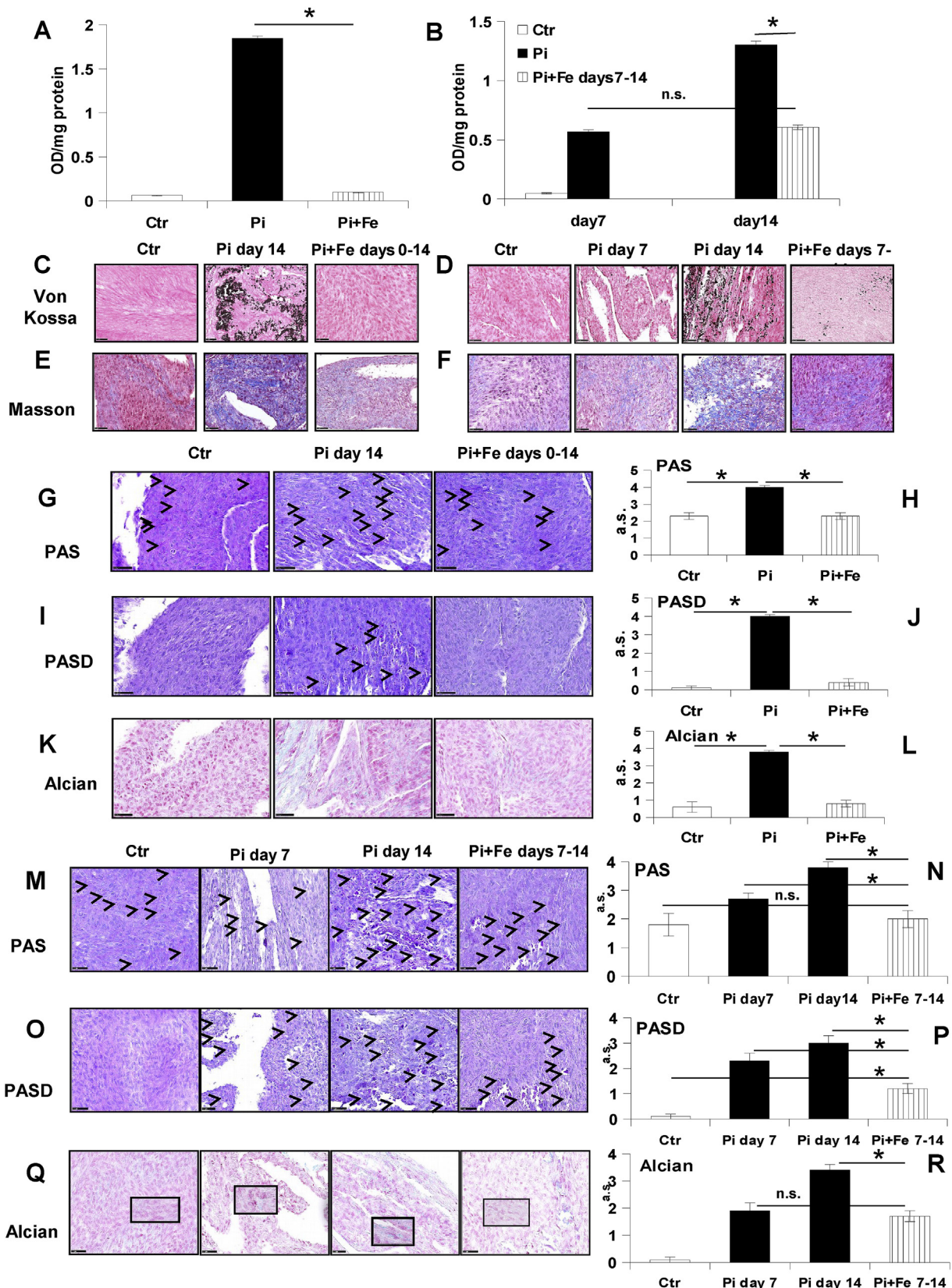


**Fig. 1.** Effect of prophylactic and therapeutic addition of iron citrate on high-Pi induced calcification, fibrosis and granule osteo-chondrogenic shift. Rat VSMCs were cultured with 5 mM Pi in the calcification medium up to 14 days. **A, B:** Calcium deposition was measured by destaining and normalized by cellular protein content. **C, D:** Ca deposition was visualized by Von Kossa staining (black). **E, F:** Masson's stainings, VSMCs appear in red whereas collagen fibers are in blue. **G, I, M, O:** arrows indicate granules; **E, Q:** light blue indicates acid mucins. **H, J, L, N, P, R:** Semi-quantitative analysis of staining data. **A:** Pretreatment with 50  $\mu$ M Fe is able to prevent high-Pi calcium deposition at day 14. **B:** The addition of 50  $\mu$ M Fe on already calcified VSMCs from day 7 to day 14 is able to block completely the additional high-Pi calcium deposition. **C, D:** Pretreatment or treatment of already calcified VSMCs with 50  $\mu$ M Fe modifies calcium

fiber network and mechanical models of cardiovascular development, growth, and remodelling of vessels have been investigated [4]. Elevated extracellular Pi affects multiple signalling pathways leading to vascular smooth muscle cell (VSMC) trans-differentiation [5] that induces VSMCs to synthesize and deposit ECM elements typical of bone thus modifying muscular ECM characteristics and arterial stiffness. The myogenic tone depends on VSMC contractility that is influenced by cell-ECM interaction. Calcification-induced arterial stiffness causes significant mechanical changes in the arterial wall with a resulting altered extensibility with increased pulse wave velocity and pressure [6].

Recently, we demonstrated the effect of iron citrate in preventing VC progression in an *in vitro* model of high-Pi induced VC. In fact, iron reduces Ca deposition through prevention of apoptosis and potentiation of autophagy [7]. In the present study, we investigated the direct effect of iron citrate in the modulation of ECM modification induced by high-Pi, following either a prophylactic or a therapeutic protocol.

## 2. Methods

### 2.1. Induction of calcification

Rat VSMCs were obtained as previously described [8], at 80% confluence cells were switched to calcification medium (CM) and challenged with 5 mM Na<sub>3</sub>PO<sub>4</sub> (Pi). For miRNA quantification, VSMCs were cultured with medium supplemented with exosome-depleted FBS by 18 h centrifugation at 120,000×g. We performed two different protocols of iron citrate (Fe) administration: prophylactic Fe administration 1 h before Pi challenge at day 0, and therapeutic Fe addition from day 7–14 of calcification.

For rat aortic rings we harvested aorta, cleaned it and cut into sections, after 24 h stabilization in growth medium (GM) they were switched to CM (3 mM Pi). All rats were kept in accordance with guidelines from Directive 2010/63/EU of the European Parliament on the protection of animals used for scientific purposes and the Italian Ministry of Health and the local University of Milan ethics committee approved the protocol (NCT03169400).

Extracellular calcium deposits were stained with Alizarin Red S solution for 30 min and destained for 24 h with 5% perchloric acid, and Ca<sup>++</sup> content was determined colorimetrically at 450 nm wavelength [8].

### 2.2. Exosome isolation and measurement of phosphate levels

Exosome isolation was performed from CM (1 ml). RNase A (6.7 µg/ml) was added for 15' RT. CM was centrifuged at 16,000×g 10' 4 °C. Exosomes were isolated with the Exosome Precipitation Solution (Macherey-Nagel) and then re-suspended in 100 µl 0.6 M HCl and left at RT for 48 h. . Exosome characterization was performed by EM (S1 Fig.A).

### 2.3. RNA extraction and RT-PCR

Total VSMC RNA [8] and miRNA were extracted using PureLink RNA Mini Kit. Exosome miRNA was extracted with NucleoSpin

miRNA Plasma kit. The relative expression of target genes was performed by ΔΔ cycle threshold method.

### 2.4. Histochemistry

VSMCs or aortic rings were formalin-fixed and paraffin-embedded. Histochemical stainings were performed as described in the AFIP manual [9]. Elastic fibers yellowish fluorescence stained in H&E was used to evaluate elastin [10]. Specifically, a) elastin fragmentation and b) the percentage of vascular wall integrity were scored: a) 1: heavy elastin fragmentation; 2: median degree of fragmentation; 3: focal discontinuity; 4 complete integrity; b) 1: <25%; 2: 25–50%; 3: 51–75%; 4: >75%. Calcium and iron deposits were visualized by Von Kossa and Perls staining as black and Prussian blue granules; glycogenic (PAS+) and non glycogenic (PASD resistant) material was appreciated as magenta granules and light blue for acid mucopolysaccharides by Alcian blue pH 1. Deposit quantification was scored: 0: no deposits; 1: few faint granules; 2: average quantity of faint granules; 3: average quantity of large granules; 4: abundant large granules. Sirius Red and Fast Green [11] stained collagen fibers evaluated as thickening and orientation, scored: a) 1: tiny and ordered fibers; 2: slight thickened, ordered fibers; 3: thickened and initially disordered fibers; 4: heavy thickened disordered fibers.

### 2.5. Sirius Red/Fast Green destaining

After fixing VSMCs with Kahle fixative 10min RT, cells were stained with Fast Green 0.1% and Sirius Red 0.04% in picric acid 1:1, 30min RT. Sirius Red and Fast Green were eluted with 0.1 N NaOH 5 min RT and analyzed at 540 nm and 605 nm, respectively. After spillover evaluation, collagen (Sirius Red) and non-collagenous proteins (Fast Green) were calculated and data presented as Sirius Red/Fast Green values.

### 2.6. Sirius Red polarization microscopy automated analysis

In Sirius-red sections positivity to collagen was quantified in 3 non-overlapping 40× areas on tunica media by ImageJ [12]. Aorta was outlined to define the region of interest (ROI), threshold set to omit background and fibrosis was calculated as the percentage of unmasked pixels above threshold, relative to total pixels within the ROI. Data are presented as % of fibrotic area.

### 2.7. Electron microscopy

VSMCs were fixed in 2.5% glutaraldehyde in 0.13 M phosphate buffer pH 7.2–7.4 for 2 h, post-fixed in 1% osmium tetroxide, dehydrated through graded ethanol and propylene oxide and embedded in epoxy resin. Ultrathin sections (50–60 nm) were counterstained with Pt-blue solution and lead citrate.

### 2.8. Statistical analysis

Results are expressed as mean ± SEM. Experiment were performed at least three times at least in triplicate. Differences were

deposition. **E, F:** Pretreatment or treatment from day 7 to day 14 with 50 µM Fe shows, at day 14, modified collagen synthesis. **G, H:** Pretreatment with 50 µM Fe prevents the high-Pi induced increase in granules (PAS staining); **I, J:** High-Pi treatment induces non-glycogen granules prevented by 50 µM Fe (PASD staining); **K, L:** The high-Pi induced increase in acidic mucins is prevented by 50 µM Fe (Alcian staining). **M, N:** Therapeutic treatment with 50 µM Fe reduces the total granule content induced by high-Pi to a lower level compared to day 7 of calcification (PAS staining); **O, P:** Therapeutic treatment with 50 µM Fe addition reduces the non-glycogen granules to a lower level as compared to day 7 of calcification (PASD staining); **Q, R:** Therapeutic treatment with 50 µM Fe addition reduces Alcian positive extracellular granule content to levels similar to that of day 7; insets show that VSMCs stop the synthesis and secretion of mucins in granules, with a reversion of the morphology that becomes similar to control VSMCs. Data are presented as mean ± SE of 3 experiments in triplicate. (\*p < 0.01). Magnification as scale bar. (For interpretation of the references to color in this figure legend, the reader is referred to the Web version of this article.)

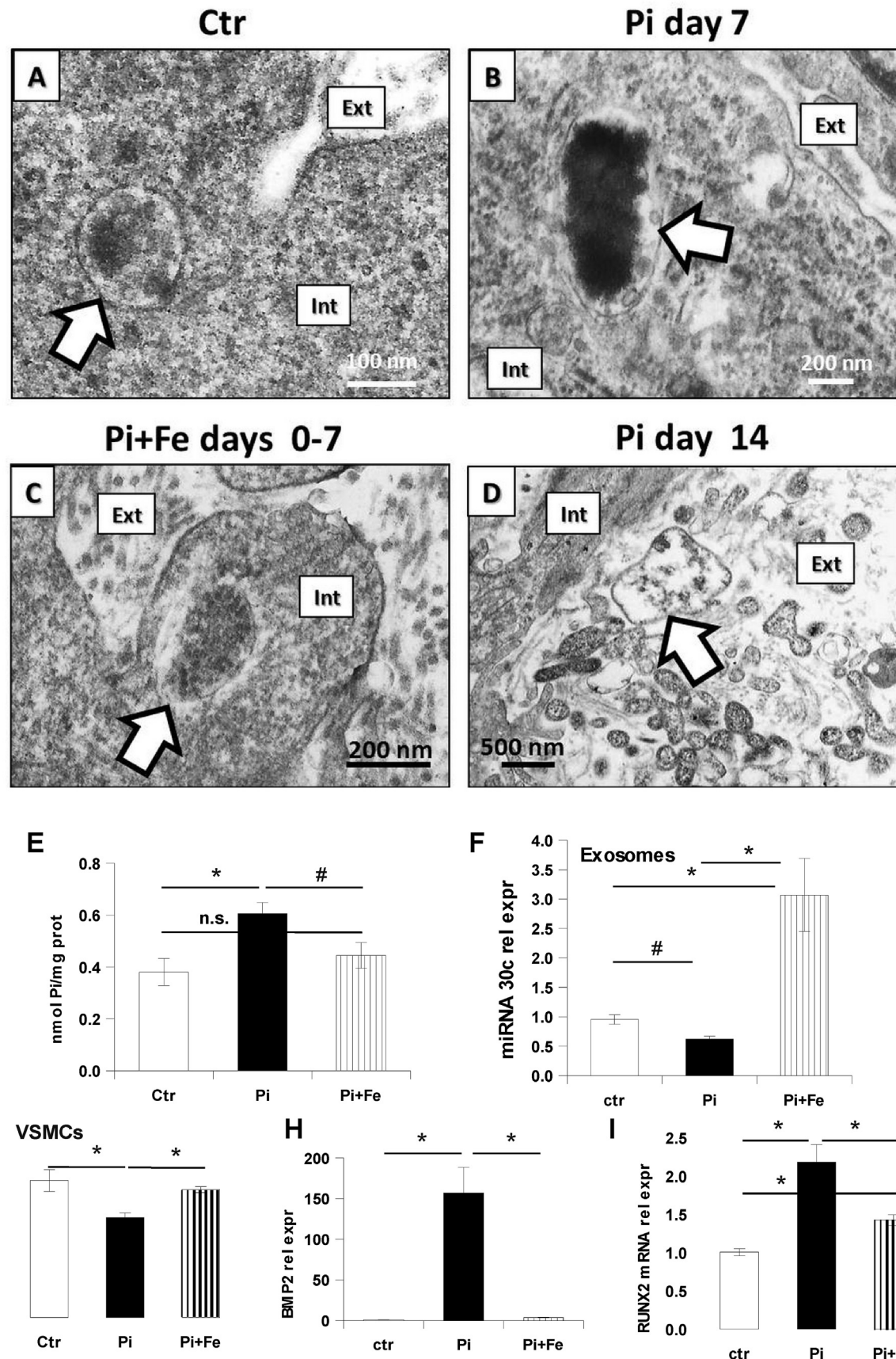


**Fig. 2.** Effect of iron citrate on high-Pi induced ECM modification and exosome composition. Rat VSMCs were cultured with 5 mM Pi in the calcification medium up to 14 days. **A–D:** Ultrastructural characteristics were visualized by EM on ultrathin sections; **E, G:** miRNA quantification by RT-PCR; **F, H:** mRNA quantification by RT-

analyzed by one-way ANOVA followed by Bonferroni post-hoc test and considered significant when  $p < 0.05$ . Score statistical analysis were evaluated by Kruskal-Wallis test corrected for ties.

### 3. Results

#### 3.1. Iron citrate prevents and blocks calcium deposition and granule osteo-chondrogenic modification induced by high-Pi in VSMCs

Analysis of Ca deposits induced by high-Pi (5 mM) in VSMCs showed 94% inhibition by iron (50  $\mu$ M Fe) added prophylactically and 53% added therapeutically, with no Ca deposition progression (Fig. 1A and B). High-Pi stimulation of VSMCs induced Ca-crystal deposition both at intra- and extra-cellular level prevented and blocked by addition iron (Fig. 1C and D). Analysis of Von Kossa staining confirmed the observations: prophylactic: ctr 0, Pi  $3.9 \pm 0.1$ , Pi + Fe  $0.1 \pm 0.1$  ( $p < 0.01$ , PivsPi + Fe, a.s., Fig. 1C); therapeutic: ctr 0, Pi day 7  $2.3 \pm 0.3$ , Pi day 14  $3.8 \pm 0.2$ , Pi + Fe days 7–14  $1.7 \pm 0.2$  ( $p < 0.01$ , Pi day 14 vs Pi + Fe days 7–14, a.s., Fig. 1D). In the therapeutic protocol, black deposits in Pi + Fe days 7–14 condition were similar to those of Pi day 7 samples. Iron citrate effect was independent from iron and citrate Pi-binding capacity and by sodium citrate *per se* (S1 Fig.B, a and b, respectively).

ECM shift from muscular to fibrotic was studied by Masson's staining that showed an evident increase of blue positivity (collagen) in high-Pi treated cells. Both iron prophylactic and therapeutic addition considerably blocked high-Pi induced collagen deposition (Fig. 1E and F). In iron-pretreated VSMCs there was a light blue cell membrane staining similar to controls in opposition with the heavy light blue deposition at intracytoplasmic and membrane level, and in the extracellular space in high-Pi VSMCs. Iron addition to 7 day high-Pi treated cells highlighted an arrest in collagen deposition, preventing the heavy collagen synthesis at 14 days (Fig. 1F).

Granule glycogenic nature was tested in VSMCs by PAS and PAS diastase (PASD) staining. High-Pi challenge induced a significant increase of PAS positive granules, with iron prevention (ctr  $2.3 \pm 0.2$ ; Pi  $4.0 \pm 0.2$ ; Pi + Fe  $2.3 \pm 0.2$ , <sup>a</sup>ctrlsPi, <sup>b</sup>PivsPi + Fe, <sup>a,b</sup> $p < 0.01$ , a.s., Fig. 1G and H). PASD staining, that digests glycogen, showed no granules in controls. Instead, high-Pi treated VSMCs showed no differences between PASD and PAS positive granules, suggesting their non-glycogenic nature (Fig. 1H–J). Interestingly, iron prevented the high-Pi induced production of non-glycogenic granules (ctr  $0.1 \pm 0.1$ ; Pi  $4.0 \pm 0.1$ ; Pi + Fe  $0.4 \pm 0.2$ , <sup>a</sup>ctrlsPi, <sup>b</sup>PivsPi + Fe, <sup>a,b</sup> $p < 0.01$ , a.s., Fig. 1I and J). Alcian Blue staining showed a faint blue on control cytoplasmatic membrane, whereas evident intra- and extra-cellular light blue granularity was present in high-Pi treated cells. In iron pre-treated VSMCs Alcian Blue stained granules were not appreciable (ctr  $0.6 \pm 0.3$ ; Pi  $3.8 \pm 0.1$ ; Pi + Fe  $0.8 \pm 0.2$ , <sup>a</sup>ctrlsPi, <sup>b</sup>PivsPi + Fe, <sup>a,b</sup> $p < 0.01$ , a.s., Fig. 1K and L).

In the therapeutic protocol PAS staining showed that iron not only prevented the increase from day 7–14 induced by high-Pi, but significantly reduced granule content compared to day 7 ( $2.0 \pm 0.3$  vs  $2.7 \pm 0.2$ ; Pi + Fe days 7–14 vs Pi day 7;  $p < 0.01$ ; a.s., Fig. 1M and N), with a content similar to controls. PASD staining highlighted that iron, in established calcification, from day 7–14 decreased granule content to an extent even lower compared to day 7 ( $1.2 \pm 0.2$  vs  $2.3 \pm 0.3$ ; Pi + Fe days 7–14 vs Pi day 7;  $p < 0.01$ ; a.s.,

Fig. 1O and P). Finally, Alcian blue staining showed that starting iron treatment from day 7 induced no additional deposition of acidic mucins (Fig. 1Q and R), with a content significantly lower compared to day 14 ( $1.7 \pm 0.2$  vs  $3.4 \pm 0.2$ ; Pi + Fe days 7–14 vs Pi day 14;  $p < 0.01$ ; a.s., Fig. 1Q and R). High-Pi treated VSMCs showed a cytoplasmic Alcian blue staining, on the contrary, in Pi + Fe VSMCs, treated from day 7–14, the sub-cellular localization of light blue deposits was on cellular membrane, with a reddish cytoplasm, suggesting a reverted VSMC phenotype similar to controls (Fig. 1Q, insets).

#### 3.2. Iron citrate prevents osteogenic granules shift induced by high-Pi

Control and 7-day iron pre-treated VSMCs have granules with a diameter around 100 nm (Fig. 2A–C), whereas in high-Pi treated cells they have 500 nm diameter, dimensions typical of glycogen and of osteoblast and chondrocyte granules, respectively (Fig. 2B). High-Pi granules are loaded with electrondense material and were present both at intra end extra-cellular level (Fig. 2D). Exosomes phosphate levels increased in high-Pi samples and decreased after iron pre-treatment (ctr  $0.38 \pm 0.05$ ; Pi  $0.61 \pm 0.04$ ; Pi + Fe  $0.45 \pm 0.05$ , <sup>a</sup>ctrlsPi, <sup>b</sup>PivsPi + Fe, <sup>a</sup> $p < 0.01$  <sup>b</sup> $p < 0.05$ , nmol Pi/mg protein, Fig. 2E). MiRNA characterize exosomes and we studied miRNA 30c since it negatively regulates RUNX2 mRNA expression, the master-gene of osteoblastic differentiation. miRNA 30c decreased in high-Pi samples both in secreted exosomes and in VSMCs ( $0.95 \pm 0.08$  vs  $0.62 \pm 0.05$ ; exosomes;  $p < 0.05$ ,  $1.01 \pm 0.08$  vs  $0.74 \pm 0.03$ ; VSMCs; ctrlvsPi; relative expression,  $p < 0.01$ ; Fig. 2F and G). Interestingly, iron pretreatment was able to induce a significant increase of miRNA 30c over the control in secreted exosomes ( $0.95 \pm 0.08$  vs  $3.07 \pm 0.62$ ; ctrlvsPi + Fe,  $p < 0.01$ , relative expression, Fig. 2F). Studying the miRNA 30c regulator (BMP2) and target gene (RUNX2) in VSMCs, we found that iron prevented both high-Pi induced BMP2 and RUNX2 increase ( $157.0 \pm 31.5$  vs  $3.7 \pm 0.2$  and  $2.2 \pm 0.2$  vs  $1.4 \pm 0.1$ ; PivsPi + Fe; BMP2 and RUNX2; relative expression,  $p < 0.01$ ; Fig. 2H and I).

#### 3.3. Iron citrate both prevents and blocks or partially reverts calcium deposition, fibrosis and elastinolysis induced by high-Pi in aortic rings

First, we evaluated calcium deposition *ex vivo* finding a prevention or block by iron (100  $\mu$ M) (Fig. 3A). In fact, Von Kossa staining showed: prophylactic: ctr 0, Pi  $4.0 \pm 0.2$ , Pi + Fe  $1.5 \pm 0.5$  ( $p < 0.05$ , PivsPi + Fe, a.s., day 14, Fig. 3B) and no black calcium deposits in Pi + Fe VSMCs were detectable. In the therapeutic protocol, there was an iron-induced arrest in calcium deposition: ctr 0, Pi day 7  $2.0 \pm 0.2$ , Pi day 14  $4.0 \pm 0.2$ , Pi + Fe days 7–14  $3 \pm 0.1$  ( $p < 0.05$ , Pi day 14 vs Pi + Fe days 7–14, a.s., Fig. 3C). Iron treatment induced iron deposition in aortic tissue (Fig. 3D and E).

Seven day high-Pi treated VSMCs showed fibrosis with fibrils thickened and disorganized with a dense connective tissue structure with iron-pretreatment preserving collagen fibrils structure similar to controls (Fig. 3G and H). Fig. 3I and J shows that ECM is rich of collagen fibrils that serve as scaffold for calcium crystal nucleation.

Aortic rings were stained with Sirius Red/Fast Green (Fig. 3K and

PCR. E–I day 10. **Int:** intracytoplasmic compartment; **Ext:** extracytoplasmic compartment. **A:** Intracytoplasmic vesicle (arrow) containing glycogen in control VSMCs. Scale bar 100 nm; **B:** High-Pi induces the formation of intracytoplasmic vesicle (arrow) containing electrondense material. - Scale bar 200 nm; **C:** Pretreatment with 50  $\mu$ M Fe preserves glycogen intracytoplasmic vesicle (arrow). Scale bar 200 nm; **D:** High-Pi treatment induces MVs (arrow) formation and their secretion in the extracellular compartment. Scale bar 500 nm; **E:** In culture medium-isolated exosomes 50  $\mu$ M Fe prevents high-Pi induced increase in phosphate content. **F, G:** 50  $\mu$ M Fe prevents high-Pi induced decrease in miRNA 30c in culture-medium isolated exosomes and VSMCs. **H, I:** In VSMCs 50  $\mu$ M Fe prevents high-Pi induced increase in BMP2 and RUNX2 mRNA. Data are presented as mean  $\pm$  SE of 3 experiments in triplicate. (# $p < 0.05$ ; \* $p < 0.01$ ).

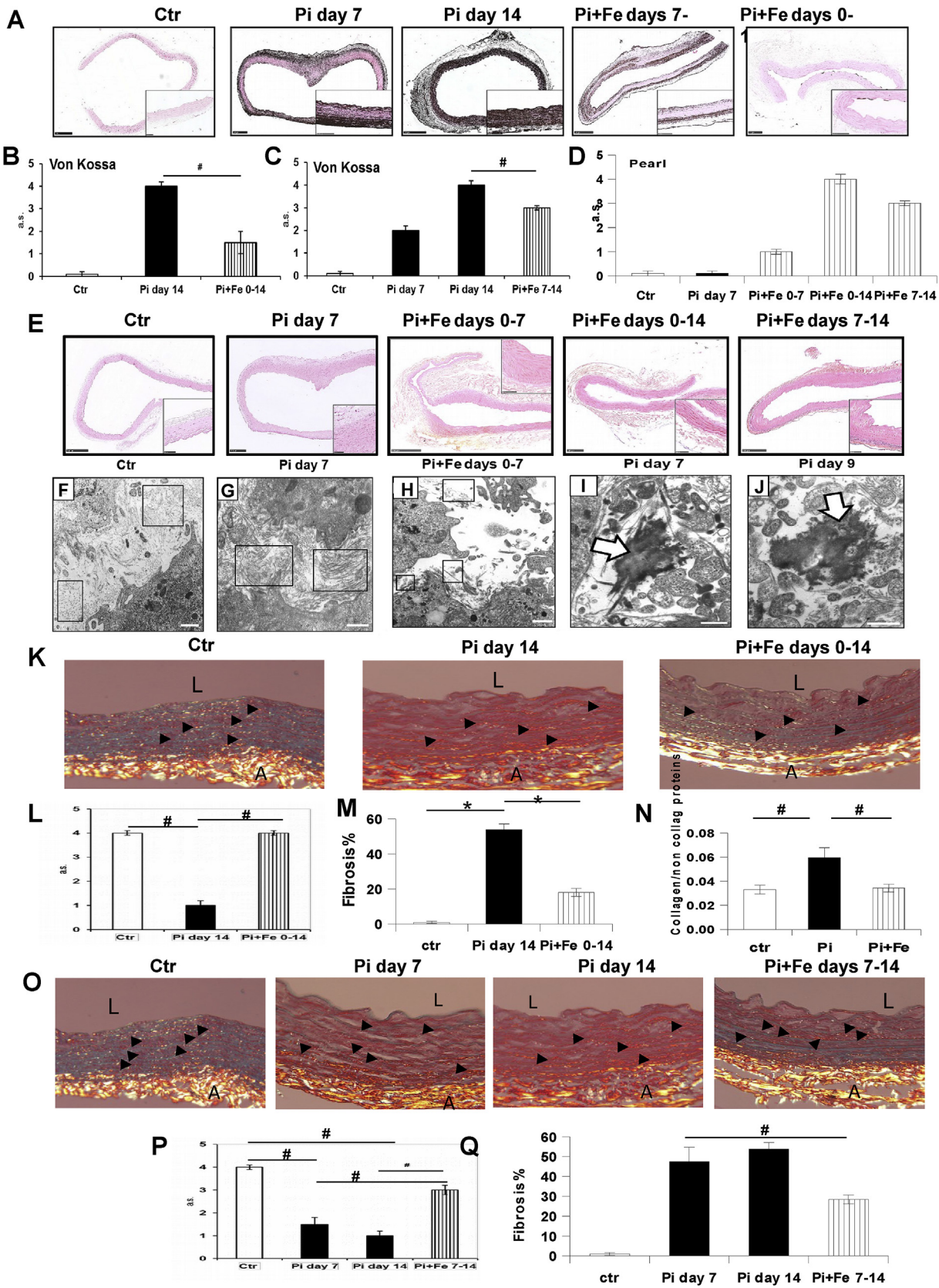


**Fig. 3.** Effect of prophylactic and therapeutic addition of iron citrate on high-Pi induced calcification, fibrosis and iron accumulation in aortic rings. Rat aortic rings were incubated with 3 mM Pi in the calcification medium up to 14 days. **A:** Calcium deposits were visualized in black by Von Kossa staining; **E:** Iron deposits were visualized in light blue by Perls staining; **F–J:** Ultrastructural characteristics were visualized by EM on ultrathin sections; **K–O:** Collagen was visualized by polarization contrast microscopy after Sirius Red and Fast Green staining (L lumen, A tunica adventitia); **M, Q:** Fibrosis percentage by automated analysis. **N:** Sirius Red/Fast Green destaining data. **B, C, D, L, P:** Semi-quantitative analysis of staining data. **A, B, C:** The addition of 100  $\mu$ M Fe either prophylactically or therapeutically either prevent or delay the additional high-Pi calcium deposition after 14 days. **D, E:** Iron

N). Control rings showed radial organized tight and tidy collagen fibrils that after high-Pi become disorganized with presence of thick fibrils, haphazard mass of collagen and elastin fragmentation ( $4.0 \pm 0.1$  vs  $1.0 \pm 0.2$  day 14; structure; ctrvsPi, a.s., p < 0.05; Fig. 3L). Iron prophylactic treatment preserved collagen organization and structure similar to controls ( $1.0 \pm 0.2$  vs  $4.0 \pm 0.1$  day 14; structure; Pi vs Pi + Fe, a.s., p < 0.05; Fig. 3L). Moreover, iron prevented high-Pi induced fibrosis ( $53.9 \pm 3.2$  vs  $18.1 \pm 2.2$ ; PivsPi + Fe, fibrosis %, p < 0.01; Fig. 3M). Sirius Red/Fast Green destaining on VSMCs confirmed a high-Pi induced collagen synthesis prevented by iron (ctr  $0.033 \pm 0.004$ ; Pi  $0.060 \pm 0.008$ ; Pi + Fe  $0.034 \pm 0.003$ , <sup>a</sup>ctrvsPi, <sup>b</sup>PivsPi + Fe, <sup>ab</sup>p < 0.05, collagen/non-collagenous proteins, Fig. 3N). Considering the Pi/ctr ratio there is a high-Pi induced increase over the control of 1.80, prevented by iron (1.03 Pi + Fe/ctr ratio).

Iron addition, when calcification was already established, protected the aortic wall from progression of high-Pi induced fibrosis ( $1.0 \pm 0.2$  vs  $3.0 \pm 0.2$ ; structure; Pi day 14 vs Pi + Fe days 7–14; a.s., p < 0.05; Fig. 3O and P) and promoted an apparent fibril rearrangement and block of high-Pi induced thickening of collagen fibrils ( $1.5 \pm 0.3$  vs  $3.0 \pm 0.2$ ; structure; Pi day 7 vs Pi + Fe days 7–14; a.s., p < 0.05; Fig. 3P). Moreover, not only there was less fibrosis in iron-treated rings from day 7–14 compared with 14 days of high-Pi, but there was also a regression compared to day 7 ( $53.9 \pm 3.2$  vs  $28.4 \pm 2.2$  and  $47.5 \pm 7.3$  vs  $28.4 \pm 2.2$ ; Pi day 14 vs Pi + Fe days 7–14 and Pi day 7 vs Pi + Fe days 7–14; fibrosis %, p < 0.05; Fig. 3Q).

We next evaluated iron effect on high-Pi induced elastin damage that is characterized by elastin discontinuity and fragmentation ( $4.0 \pm 0.1$  vs  $1.5 \pm 0.5$ ; distribution;  $4.0 \pm 0.1$  vs  $1.5 \pm 0.5$ ; structure; ctrvsPi, a.s., p < 0.05; Fig. 4A and B). Interestingly, the damage was prevented by iron ( $1.5 \pm 0.5$  vs  $4.0 \pm 0.3$ ; distribution;  $1.5 \pm 0.5$  vs  $3.0 \pm 0.2$ ; structure; PivsPi + Fe; a.s., p < 0.05; Fig. 4B and C). Evaluation of elastin mRNA levels in VSMCs demonstrated a decrease of elastin synthesis after high-Pi treatment prevented by iron (ctr  $1.0 \pm 0.1$ ; Pi  $0.7 \pm 0.1$ <sup>\*</sup>; Pi + Fe  $1.2 \pm 0.1$ <sup>#</sup>, \*ctrvsPi, #PivsPi + Fe, p < 0.05, relative expression, p < 0.05; Fig. 4D).

Iron addition on established calcification protected aortic wall from high-Pi induced progression of elastinolysis ( $1.5 \pm 0.5$  vs  $3.5 \pm 0.4$ ; distribution;  $1.5 \pm 0.5$  vs  $4.0 \pm 0.2$ ; structure; Pi day 14 vs Pi + Fe days 7–14; a.s., p < 0.05; Fig. 4F and G) and reverted the high-Pi induced damages ameliorating the elastic structure of the vessel wall compared to day 7 ( $3.0 \pm 0.2$  vs  $4.0 \pm 0.2$ ; structure; Pi day 7 vs Pi + Fe days 7–14; a.s., p < 0.05; Fig. 4C–G).

#### 4. Discussion

CKD patients frequently develop VC, defined as an inappropriate pathological deposition of calcium crystals in the vasculature. VSMCs actively participate in hydroxyapatite deposition in the extracellular matrix (ECM), caused by their simil-osteoblastic trans-differentiation induced by high-Pi [1]. One of the main consequences of VSMC phenotypic switch is the modification of ECM characteristics that lead to arterial stiffness.

We studied some characteristics of the main components of tunica media namely collagen and elastic fibers, VSMCs and proteoglycans during VC [13]. Recently, we demonstrated an anti-

calcific effect of iron citrate in an *in vitro* model of high-Pi induced calcification [7]. The interest in iron salts is legitimate by the recent clinical use of iron citrate and sucroferric oxyhydroxide to manage hyperphosphatemia in CKD [14]. In particular, iron citrate as phosphate binder demonstrated efficacy and safety in dialysis patients, ameliorating anaemia and reducing intravenous iron and erythropoietin-stimulating agent use [15].

In this study we utilize iron citrate 50 or 100  $\mu$ M corresponding to a range between 2.7 and 5.4 mg Fe/L, concentrations at least one order of magnitude lower compared to plasmatic iron concentration obtained by an intravenous administration of iron [16]. Iron citrate prevents and blocks calcium deposition not only in VSMCs [7], but also in rat aortic ring and this effect is independent by its phosphate binding capacity since Pi concentration in the medium is not affected by iron citrate addition. In bone, hydroxyapatite nucleation is mediated by matrix vesicles (MVs) [17], whereas trans-differentiated VSMCs probably deposit calcium crystals through apoptotic bodies (AB) [18]. VSMCs are rich in glycogen granules [19]. Stimulation with high-Pi induced a change in granule content and profile, granules resemble MVs for their bigger size [20]. This change in dimension is prevented by iron addition with granules similar to control granules in Pi + Fe samples. Iron is also able to modulate phosphate exosome content, preventing the increase in phosphate load induced by high-Pi. Moreover, when calcification is already established, iron reverses the process of granule transformation with less MVs, smaller size, typical of glycogen granules. An explanation of this effect can be found considering that iron inhibits apoptosis in VSMCs [7] and likely inhibits ABs secretion in the extracellular compartment and in turn inhibits calcium phosphate release and ECM calcification. In fact, diastase resistance and Alcian-blue staining of high-Pi treated VSMCs support an osteo-chondrogenic shift, which is prevented by iron. Interestingly, we also demonstrate an effect of iron on established calcification in reverting the nature of granules and proteoglycans and in decreasing MV production, suggesting that it may be possible to block and partially revert ECM osteo-chondrogenic shift. To better characterize osteo-chondrogenic granule shift we studied miRNAs [21] content in exosomes. It has been demonstrated that BMP2 downregulates miRNA 30c to increase RUNX2 expression in a model of VC [22]. Proving the exosome shift towards an osteogenic type, miRNA 30c decreases in exosomes from high-Pi treated VSMC with a corresponding increase in RUNX2 mRNA levels probably due to BMP2 increase. Surprisingly, iron pretreated exosomes show an increase in miRNA 30c and a RUNX2 decrease. Thus, one of iron mechanism of VC prevention might be the active modulation of exosome miRNA content to inhibit VSMC osteoblastic transformation. By Masson's staining we found an increase in fibrosis in high-Pi stimulated VSMC with more intense blue staining, both in the cytoplasm and ECM, characteristics modified by iron. In fact, in iron prophylactic treatment the staining features are maintained similar to controls, and in therapeutic samples, iron addition, to already calcified VSMCs, stopped the blue staining to the intermediate cellular characteristics of day 7, when initial modification towards fibrotic changes can be appreciated. We then studied collagen as a constitutive element of vascular ECM since collagen scaffold architecture is crucial to the proper mechanical

addition both in the prophylactic and the therapeutic protocol induced iron deposition. F: Collagen fibers (boxed areas) in control VSMC ECM disposed in a loose network; G: Densely packed bundles of collagen fibers (boxed areas) in high-Pi treated VSMCs; H: Pretreatment with 100  $\mu$ M Fe preserves collagen fibers (boxed areas) organization in a loose network in ECM; I, J: High-Pi treatment induces microcalcification in the ECM associated to collagen fibers (arrows). K, L: the high-Pi induced disorganization and thickening of collagen fibrils is prevented by 50  $\mu$ M Fe; M: Pretreatment with 100  $\mu$ M Fe protects the artery wall from the high-Pi induced increase in fibrosis. N: VSMC 14 days treatment with 100  $\mu$ M Fe prevents high-Pi induced increase in collagen deposition. O, P: Therapeutic addition of 100  $\mu$ M Fe partially reverts high-Pi induced disorganization and thickening of collagen fibrils. Q: Iron citrate therapeutically reverts the fibrosis of the artery wall induced by high-Pi treatment. Data are presented as mean  $\pm$  SE of at least 2 experiments in triplicate. (\*p < 0.01; <sup>#</sup>p < 0.05). Magnification  $\times 40$ . F–J scale bar 500 nm. (For interpretation of the references to color in this figure legend, the reader is referred to the Web version of this article.)

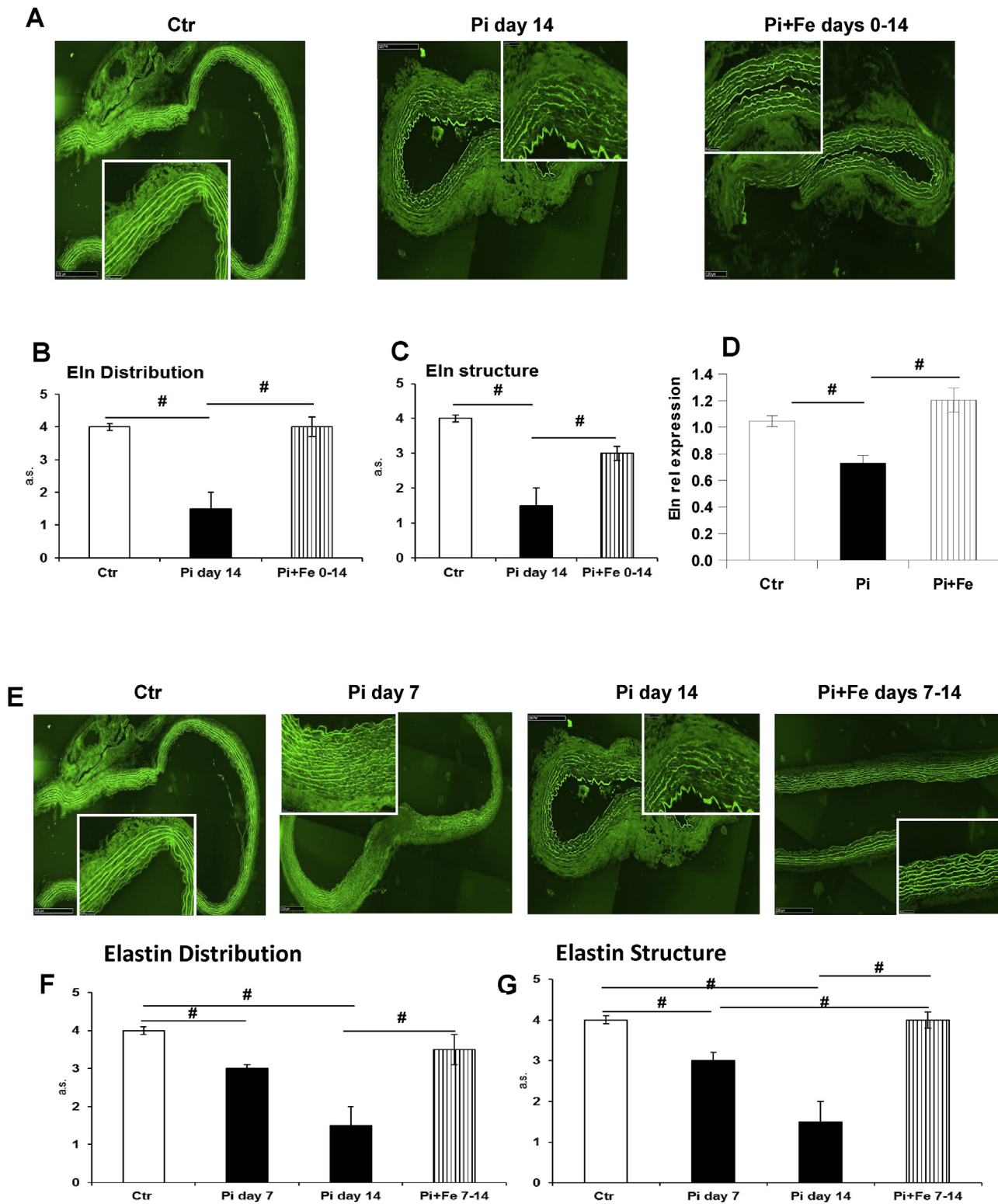


**Fig. 4.** Effect of prophylactic and therapeutic addition of iron citrate on high-Pi induced elastinolysis. Rat aortic rings were incubated with 3 mM Pi in the calcification medium for 14 days. **A, E:** Elastin was visualized in green fluorescence by Hematoxylin and Eosin staining; **D:** Elastin mRNA quantification by RT-PCR; **B, C, F, G:** Semi-quantitative analysis of staining data. **A, B, C:** High-Pi elastin fragmentation and discontinuity within the aortic wall is prevented by 100  $\mu$ M Fe. **D:** VSMC treatment for 8 days with 100  $\mu$ M Fe is able to prevent high-Pi induced decrease in elastin mRNA. **E:** Therapeutic addition of 100  $\mu$ M Fe is able to revert high-Pi induced fragmentation and discontinuity within the aortic wall. **F, G:** Addition of 100  $\mu$ M Fe to already calcified aortic rings is able to protect the vessel from the high-Pi induced elastin fragmentation in aortic rings. Data are presented as mean  $\pm$  SE of 2 experiments in triplicate. (# $p < 0.05$ ). Magnification as scale bar. . (For interpretation of the references to color in this figure legend, the reader is referred to the Web version of this article.)

functioning of arteries.

In aortic rings, high-Pi treatment induced a disorganization and thickening of collagen fibrils with an increase of haphazard mass of collagen and elastin fragmentation. Iron pretreatment preserved the fibril collagen organization preventing fibrosis in aortic rings (~66%). Iron on already calcified aortic rings was able to promote a reorganization of collagen fibrils with a setting similar to control vessels resulting in the regression of fibrosis (~40%). Since collagen fibrils function as scaffold for calcium crystal nucleation, the effect of iron on collagen is relevant in its anti-calcific action. In fact, there has been identification of signalling pathways of collagen cross-linking and bone mineralization as potential new targets for VC in CKD patients with atherosclerosis [23]. Moreover, Jover et al. demonstrated the importance of enzymes involved in collagen cross-linking to ECM to play a key role during high-Pi induced VSMC calcification [24].

Elastin is secreted by VSMCs and constitute elastic lamellae that are fundamental for the extensive tensile strength of vessels and elastin degradation is important as trigger for VC progression [25,26]. In aortic rings, iron pre-treatment has protective effect on high-Pi induced elastic lamellae degradation preventing elastin synthesis decrease. Iron treatment of established calcified aortic rings induces the restoration of the elastic lamellae structure. Iron effect in protecting elastic lamellae participate in its anti-calcific action since elastinolysis increases elastin calcium affinity [27]. The relevance of elastinolysis in CKD is demonstrated by the evidence that in uremic patients disruption of internal elastic lamina occurs in elastic arteries [28] and that there is thinning and fragmentation of medial elastic fibers [29]. Thus, the iron action on elastinolysis contribute in contrasting high-Pi induced calcification, even though elastinolysis is an early event necessary but not sufficient to induce VC [30].

In conclusion, we found that iron citrate prevents and modulates high-Pi induced ECM osteo-chondrogenic shift, acting on different factors that influence matrix properties such as granule nature, proteoglycans, collagen, and elastin. In addition to preventing the osteo-chondrogenic modification of ECM, added when calcification is already established and VSMCs are already trans-differentiated, iron citrate is able to redirect ECM characteristics towards muscular ECM and to block calcium crystal deposition. Being increase in fibrosis and in arterial stiffness relevant for cardiovascular complication, morbidity, and mortality in CKD patients, the iron effect in preventing osteo-chondrogenic ECM modification should deserve attention and further investigation.

## Contributor Roles

PC contributes to conceptualization, data curation, formal analysis, investigation, writing original draft preparation; MF, DT, CM, GB contribute to investigation; GB and PG contribute to writing review and editing; MC contributes to conceptualization, data curation, formal analysis, funding acquisition, supervision, validation, writing original draft preparation.

## Declaration of competing interest

The results presented in this paper have not been published previously in whole or part, except in abstract format. GAB received speaker honoraria from Keryx. MC and GAB participated in advisor boards with Keryx.

## Appendix A. Supplementary data

Supplementary data to this article can be found online at <https://doi.org/10.1016/j.ijcard.2019.09.068>.

## References

- [1] M. Vervloet, M. Cozzolino, Vascular calcification in chronic kidney disease: different bricks in the wall? *Kidney Int.* 91 (2017) 808–817, <https://doi.org/10.1016/j.kint.2016.09.024>.
- [2] A.N. Kapustin, M.L. Chatrou, I. Drozdov, Y. Zheng, S.M. Davidson, D. Soong, et al., Vascular smooth muscle cell calcification is mediated by regulated exosome secretion, *Circ. Res.* 116 (2015) 1312–1323, <https://doi.org/10.1161/CIRCRESAHA.116.305012>.
- [3] J.D. Humphrey, E.R. Dufresne, M.A. Schwartz, Mechanotransduction and extracellular matrix homeostasis, *Nat. Rev. Mol. Cell Biol.* 15 (2014) 802–812, <https://doi.org/10.1038/nrm3896>.
- [4] J.E. Wagenseil, R.P. Mecham, Vascular extracellular matrix and arterial mechanics, *Physiol. Rev.* 89 (2009) 957–989, <https://doi.org/10.1152/physrev.00041.2008>.
- [5] J.A. Leopold, MicroRNAs regulate vascular medial calcification, *Cells* 3 (2014) 963–980, <https://doi.org/10.3390/cells3040963>.
- [6] A. Covic, M. Vervloet, Z.A. Massy, P.U. Torres, D. Goldsmith, V. Brandenburg, et al., Bone and mineral disorders in chronic kidney disease: implications for cardiovascular health and ageing in the general population, *Lancet Diabetes Endocrinol* 6 (2018) 319–331, [https://doi.org/10.1016/S2213-8587\(17\)30310-8](https://doi.org/10.1016/S2213-8587(17)30310-8).
- [7] P. Ciceri, F. Elli, P. Braidotti, M. Falleni, D. Tosi, G. Bulfamante, et al., Iron citrate reduces high phosphate-induced vascular calcification by inhibiting apoptosis, *Atherosclerosis* 254 (2016) 93–101, <https://doi.org/10.1016/j.atherosclerosis.2016.09.071>.
- [8] P. Ciceri, E. Volpi, I. Brenna, L. Arnaboldi, L. Neri, D. Brancaccio, et al., Combined effects of ascorbic acid and phosphate on rat VSMC osteoblastic differentiation, *Nephrol. Dial. Transplant.* 27 (2012) 122–127, <https://doi.org/10.1093/ndt/gfr284>. Epub 2011 May 25.
- [9] L.G. Luna, *Manual of Histologic Staining Methods of the Armed Forces Institute of Pathology*, McGraw-Hill Book Company, 1970.
- [10] Y.S. Heo, H.J. Song, Characterizing cutaneous elastic fibers by eosin fluorescence detected by fluorescence microscopy, *Ann. Dermatol.* 23 (2011) 44–52, <https://doi.org/10.5021/ad.2011.23.1.44>.
- [11] C. Segnani, C. Ippolito, L. Antonioli, C. Pellegrini, C. Blandizzi, A. Dolfi, et al., Histochemical detection of collagen fibers by Sirius Red/Fast Green is more sensitive than van Gieson or Sirius Red alone in normal and inflamed rat colon, *PLoS One* 16 (12) (2015) 10, <https://doi.org/10.1371/journal.pone.0144630>.
- [12] J. Schindelin, I. Arganda-Carreras, E. Frise, V. Kaynig, M. Longair, T. Pietzsch, et al., Fiji: an open-source platform for biological-image analysis, *Nat. Methods* 9 (2012) 676–682, <https://doi.org/10.1038/nmeth.2019>.
- [13] M.K. O'Connell, S. Murthy, C.A. Taylor, The three-dimensional micro- and nanostructure of the aortic medial lamellar unit measured using 3D confocal and electron microscopy imaging, *Matrix Biol.* 27 (2008) 171–181, <https://doi.org/10.1016/j.matbio.2007.10.008>.
- [14] A.L. Negri, P.A. Ureña Torres, Iron-based phosphate binders: do they offer advantages over currently available phosphate binders? *Clin Kidney J* 8 (2015) 161–167, <https://doi.org/10.1093/ckj/sfu139>.
- [15] J.B. Lewis, M. Sika, M.J. Koury, P. Chuang, G. Schulman, M.T. Smith, F.C. Whittier, D.R. Linfert, C.M. Galphin, B.P. Athreya, A.K. Nossuli, I.J. Chang, S.S. Blumenthal, J. Manley, S. Zeig, K.S. Kant, J.J. Olivero, T. Greene, J.P. Dwyer, Collaborative Study Group, Ferric citrate controls phosphorus and delivers iron in patients on dialysis, *J. Am. Soc. Nephrol.* 26 (2) (2015 Feb) 493–503, <https://doi.org/10.1681/ASN.2014020212>.
- [16] P. Geisser, S. Burckhardt, The pharmacokinetics and pharmacodynamics of iron preparations, *Pharmaceutics* 3 (2011) 12–33, <https://doi.org/10.3390/pharmaceutics3010012>.
- [17] E.E. Golub, Biominerization and matrix vesicles in biology and pathology, *Semin. Immunopathol.* 33 (2011) 409–417, <https://doi.org/10.1007/s00281-010-0230-z>.
- [18] D. Proudfoot, J.N. Skepper, L. Hegyi, M.R. Bennett, C.M. Shanahan, P.L. Weissberg, Apoptosis regulates human vascular calcification in vitro: evidence for initiation of vascular calcification by apoptotic bodies, *Circ. Res.* 87 (2000) 1055–1062.
- [19] I. Marchand, K. Chorneyko, M. Tarnopolsky, S. Hamilton, J. Shearer, J. Potvin, et al., Quantification of subcellular glycogen in resting human muscle: granule size, number, and location, *J. Appl. Physiol.* 93 (2002) 1598–1607, <https://doi.org/10.1152/japplphysiol.00585.2001>.
- [20] A. Bakshian Nik, J.D. Hutcheson, E. Aikawa, Extracellular vesicles as mediators of cardiovascular calcification, *Front Cardiovasc Med* 11 (2017) 4–78, <https://doi.org/10.3389/fcvm.2017.00078>.
- [21] C. Zhang, K. Zhang, F. Huang, Exosomes, the message transporters in vascular calcification, *J. Cell Mol. Med.* 22 (2018) 4024–4033, <https://doi.org/10.1111/jcmm.13692>.
- [22] J.A. Balderman, H.Y. Lee, C.E. Mahoney, Bone morphogenetic protein-2 decreases microRNA-30b and microRNA-30c to promote vascular smooth muscle cell calcification, *J Am Heart Assoc* (6) (2012), <https://doi.org/10.1161/JAHA.112.003905>. Dec 1.
- [23] A.V. Shindyapina, G.V. Mkrtchyan, T. Gneteeva, S. Buiucli, B. Tanckowny, M. Kulka, et al., Mineralization of the connective tissue: a complex molecular process leading to age-related loss of function, *Rejuvenation Res.* 17 (2014) 116–133, <https://doi.org/10.1089/rej.2013.1475>.

- [24] E. Jover, A. Silvente, F. Marín, Inhibition of enzymes involved in collagen cross-linking reduces vascular smooth muscle cell calcification, *FASEB J.* 32 (2018) 4459–4469, <https://doi.org/10.1096/fj.201700653R>.
- [25] D.W. Urry, Neutral sites for calcium ion binding to elastin and collagen: a charge neutralization theory for calcification and its relationship to atherosclerosis, *Proc. Natl. Acad. Sci. U. S. A.* 68 (1971) 810–814, <https://doi.org/10.1073/pnas.68.4.810>.
- [26] A.S. Pai, C.M. Giachelli, Matrix remodeling in vascular calcification associated with chronic kidney disease, *J. Am. Soc. Nephrol.* 21 (2010) 1637–1640, <https://doi.org/10.1681/ASN.2010040349>.
- [27] R.B. Rucker, Calcium binding to elastin, *Adv. Exp. Med. Biol.* 48 (1974) 185–209.
- [28] L.S. Ibels, A.C. Alfrey, W.E. Huffer, P.W. Craswell, J.T. Anderson, R. Weil 3rd, Arterial calcification and pathology in uremic patients undergoing dialysis, *Am. J. Med.* 66 (1979) 790–796.
- [29] A.W. Chung, H.H. Yang, J.M. Kim, M.K. Sigrist, E. Chum, W.A. Gourlay, et al., Upregulation of matrix metalloproteinase-2 in the arterial vasculature contributes to stiffening and vasomotor dysfunction in patients with chronic kidney disease, *Circulation* 120 (2009) 792–801.
- [30] A. Pai, E.M. Leaf, M. El-Abbadi, C.M. Giachelli, Elastin degradation and vascular smooth muscle cell phenotype change precede cell loss and arterial medial calcification in a uremic mouse model of chronic kidney disease, *Am. J. Pathol.* 178 (2011) 764–773, <https://doi.org/10.1016/j.ajpath.2010.12.016>.